

Presence of unsaturated sphingomyelins and changes in their composition during the life cycle of the moth *Manduca sexta*

D. T. U. Abeytung,^{*} James J. Glick,^{*} Nicholas J. Gibson,[†] Lynne A. Oland,[†] Arpad Somogyi,^{*} Vicki H. Wysocki,^{*} and Robin Polt^{1,*}

Department of Chemistry,^{*} and Arizona Research Laboratories, Division of Neurobiology,[†]
The University of Arizona, Tucson, AZ 85721

Abstract NMR and electrospray ionization tandem mass spectrometry were used to show for the first time the presence of sphingomyelins in extracts of the tobacco hornworm *Manduca sexta* (Lepidoptera). The sphingosine in the ceramide was identified as tetradecasphing-4-enine, and the fatty acids were C18:0, C20:0, C22:0, and C24:0 (compound 1). Heterogeneity in the ceramide was observed in sphingomyelins from *M. sexta*. All of the sphingomyelins were associated with their doubly unsaturated sphingosine, tetradecasphing-4,6-dienine (compound 2), which contained the same set of fatty acids as compound 1 and represents a novel set of sphingomyelins not previously reported in Lepidoptera. Lipid rafts were isolated from brains of *M. sexta*, and the association of these novel sphingomyelins with rafts was confirmed. The existence of the additional double bond was also observed in ceramide and ceramide phosphoethanolamine isolated from *M. sexta*. The levels of the doubly unsaturated ceramide showed modest changes during metamorphosis of *M. sexta*. These results suggest that *Manduca* sphingomyelins may participate in the formation of lipid rafts, in keeping with their function in vertebrates.—Abeytung, D. T. U., J. J. Glick, N. J. Gibson, L. A. Oland, A. Somogyi, V. H. Wysocki, and R. Polt. **Presence of unsaturated sphingomyelins and changes in their composition during the life cycle of the moth *Manduca sexta*. *J. Lipid Res.* 2004. 45: 1221–1231.**

Supplementary key words ceramide • sphingosine • phosphoethanolamine • raft • apoptosis • unsaturation • olefin • alkene

Interest in insect sphingosines as cell membrane constituents dates back to the 1960s (1), but three decades of work has provided information on this class of compounds for only a few insect species, namely, *Musca domestica* (2), *Calliphora erythrocephala* (3), *Trogoderma granarium* (4), *Apis mellifera* (5), and *Aedes albopictus* (6). Similarly, only limited information exists with regard to insect gly-

cosphingolipids (GSLs, arthrosides). The mosquito *Aedes aegypti* (7), the green-bottle fly *Lucilia caesar* (8), the blowfly *Calliphora vicina* (9), and *Drosophila melanogaster* (10) have been studied, with no report of sphingomyelin in these species. Sphingomyelin is commonly found in small amounts as a cell membrane component in mammals and is present in myelinated nerve fibers in larger amounts, but its exact functions have yet to be elucidated in insects. Because ceramides and sphingosine-1-phosphate have been identified as important regulators of apoptosis, cell motility, and raft formation in mammals (11, 12), the absence of such molecules in insects would have serious implications, inasmuch as biochemical pathways in insects and vertebrates have generally been conserved over tens of millions of years.

In his review on insect glycolipids, Wiegandt (13) stated that insect ceramides typically consist of C14:1 and C16:1 sphingosines, which are shorter than mammalian bases of 18 carbons or longer. The fatty acids reported at that time were C18:0, C20:0, and C22:0. The sphingolipids isolated from *Dipteran* differed from vertebrate sphingolipids, and the presence of sphingomyelin was not reported.

The characterization of sphingosine derivatives is challenging, inasmuch as they typically constitute far less than 1% of the total lipid content of a tissue sample (14). Previously, time-consuming chemical decomposition methods and chemical derivatization were required for structural elucidation of the lipid and phospholipids of *Manduca sexta* (15). More recently, electrospray ionization-tandem mass spectrometry (ESI-MS/MS) was employed by Hsu

Abbreviations: CID, collision-induced dissociation; COSY, correlation spectroscopy; ESI, electrospray ionization; FAB, fast atom bombardment; FT-ICR, Fourier transform ion cyclotron resonance; GPI, glycosylphosphatidylinositol; MSⁿ, nth-order tandem mass spectrometry; TBST, tris-buffered saline; TNE, tris-sodium EDTA; TUNEL, terminal deoxynucleotidyl transferase-mediated biotin-dUTP nick end labeling.

¹ To whom correspondence should be addressed.
e-mail: polt@u.arizona.edu

Manuscript received 15 September 2003 and in revised form 2 March 2004.

Published, JLR Papers in Press, April 21, 2004.
DOI 10.1194/jlr.M300392.JLR200

Copyright © 2004 by the American Society for Biochemistry and Molecular Biology, Inc.

This article is available online at <http://www.jlr.org>

and Turk (16) to rapidly confirm the chain lengths of the sphingoid base and the fatty acid with a minimal consumption of material. Mass spectrometry seems well suited for the analysis of these minor, albeit important, membrane constituents.

Ceramide is known to play a crucial role in apoptosis (17–20). The C(4)-C(5) *E*-alkene plays a critical role in activating the allylic alcohol toward oxidation to the enone (21, 22). Introduction of an additional double bond could, in principle, activate the resulting doubly unsaturated ceramide toward oxidation and subsequent apoptosis. Sphingadienes with additional unsaturation at C-8 of the sphingosine moiety have been reported in plants and invertebrates (23–25). Ceramides with additional unsaturation at C-6 of the sphingosine chain have also been isolated from silk moth larvae (26). Ceramides with alkenes at C(5) and C(6) and conjugated dienes at C(4,6) have been synthesized (27, 28) in order to provide evidence for the role of the allylic alcohol in the apoptotic effects of ceramides in mitochondria.

In the course of the present work, a novel series of sphingomyelins not previously reported in *Lepidoptera* was isolated. Using electrospray nth-order tandem MS/MS (MS^n) techniques and 1H -NMR, the presence of 4,6-sphingadienes in the form of ceramide, sphingomyelin, and ceramide ethanolamine were confirmed in the insect *M. sexta*. Ceramides, in the form of sphingomyelin and GSLs, are components of vertebrate lipid rafts (29, 30). Rafts are distinguished from ordinary phospholipid membranes by their ability to persist in Triton X-100 at 4°C (31, 32). We speculate that the sphingomyelins may be constituents of lipid rafts in insects (33) and might play an indirect role in apoptosis and other cellular behaviors (34) by serving as a source of ceramide. Some experiments that demonstrate the plausibility of these notions are also presented.

EXPERIMENTAL PROCEDURES

Materials and equipment

1H -NMR experiments were performed on a Bruker DRX500 (500 MHz) instrument and processed using Xwinnmr (Bruker, Inc.) software. High-resolution fast atom bombardment (FAB) mass spectra were obtained using a JEOL HX110A electric/magnetic sector spectrometer, with *meta*-nitrobenzoyl alcohol as the ionization matrix. An IonSpec 4.7T Fourier transform ion cyclotron resonance (FT-ICR) instrument equipped with an ESI source was also used to perform accurate measurements and to achieve ultrahigh mass resolution. ESI mass spectra were also obtained using two additional instruments. A Finnigan ion trap (IT) LCQ classic HPLC/MS was used in positive-ion mode. Typical ESI conditions were as follows: needle voltage, 4.5 kV; capillary voltage, 20 V; capillary temperature, 200°C; flow rate with infusion, 8 μ l/min. The tandem mass spectroscopy measurements (MS^n , $n = 2$ –5) were performed in the IT with helium as a collision gas at a pressure of $\sim 10^{-5}$ torr. Samples were electrosprayed in $CHCl_3$ -methanol 1:4 solvent mixture in a concentration range of 100–150 μ M. The Finnigan TSQ-7000 triple-stage quadrupole mass spectrometer was equipped with an electrospray ion source and controlled by Finnigan XCalibur software (version 1.2). For ESI, 10 μ l of a 1 mg/ml sphingomyelin sample (~ 20 pmol/ μ l)

was combined with 50 μ l LiOAc in water from a 100 mM stock solution (final concentration 5 μ mol/ μ l) and dissolved in 940 μ l $CHCl_3$ - CH_3OH (1:4). The mass-to-charge (m/z) range of 100–1,000 daltons (μ) was scanned 1–3 min, and the spectra averaged. For the ESI collision-induced dissociation (CID) experiments, the precursor ion was mass selected with a (\pm) 0.5 μ window in Q1, and collided with argon in Q2 with an argon gas pressure of 2.39 mTorr and a laboratory collision energy of 50 eV. The m/z range of 200–500 μ in Q3 was scanned for 5–10 min and the spectra averaged. Dialysis tubing was 500 molecular weight cutoff obtained from Spectrum Laboratories, Inc. HPLC column was Platinum Silica 100 Å, 10 μ , 250 mm \times 4.6 mm, obtained from Alltech Associates, Inc. The HPLC was a Varian Instruments, Inc. system consisting of two Model 210 pumps with 25 ml pump heads, a Model 430 autosampler with a 100 μ l SS sample loop, a Model 330 photodiode array detector, a Model 704 fraction collector, and a 100 μ l SS sample loop. The system was controlled with Varian Instruments, Inc. Star Finder software, version 5.52. Sphingomyelinase was purchased from Sigma (catalog number S 8633).

Isolation of sphingosines

All *M. sexta* larvae used in the experiment were 4-day-old fifth instars raised in a laboratory colony at 25°C and 50–60% relative humidity as described previously (35). A total of 54 larvae were dissected to remove the food-containing gut. The remaining tissue was freeze dried to obtain 33 g of dried tissue, which was ground to a powder and washed with 300 ml of acetone for 5 min in a round-bottom flask. The residue was extracted into 300 ml of 2-propanol-hexane-water (55:20:25) at 50°C for 4 h, and this was repeated a second time. The combined extracts were filtered and treated with $CHCl_3$ -MeOH-0.8 M aqueous NaOAc (30:60:8) at 50°C for 4 h. Solvents were removed from the filtered extracts to obtain 8 g of the crude lipid mixture. These lipids were saponified at room temperature overnight using 30 ml of 1 M NaOH. The neutralized solution was dialyzed for 3 days against deionized water. Upon freeze drying, 1 g of yellow powder was obtained. This was passed through silica gel (20 g) and eluted first with $CHCl_3$, $CHCl_3$ -MeOH (8:2), $CHCl_3$ -MeOH- H_2O (120:70:17), and $CHCl_3$ -MeOH- H_2O (30:60:8). The first two fractions were discarded, and the third and fourth fractions were combined and rotavapped to obtain 300 mg of a yellow powder. This was passed through DEAE Sephadex using $CHCl_3$ -MeOH- H_2O (30:60:8) to obtain 290 mg of the crude sphingosine mixture. This mixture was purified with HPLC using a solvent gradient of isopropanol-hexane-water (55:44:1) to isopropanol-hexane-water (55:35:10) at a flow rate of 1 ml/min for 45 min with monitoring at 208 nm. Fractions were collected each minute using a Varian fraction collector. The fractions with a retention time of 5 min gave ceramide, 19 min gave ceramide ethanolamine, and 32 and 33 min gave sphingomyelin.

The same method was used to obtain sphingomyelin from animals at stage 12 and stage 18 of metamorphosing adult development.

TLC staining for sphingosines

Sphingomyelins and ceramides produce a brown stain with orcinol in sulfuric acid [0.2% orcinol in H_2SO_4 : H_2O (1:4)]. Ceramide ethanolamines produce a purple stain with ninhydrin. The fractions were analyzed by TLC using a mobile phase of $CHCl_3$ -MeOH- H_2O (120:70:17), resulting in R_f values of 0.92, 0.78, and 0.52 for ceramide, ceramide ethanolamine, and sphingomyelin, respectively, on Whatman K5F silica gel 150 Å (catalog number 4851-320).

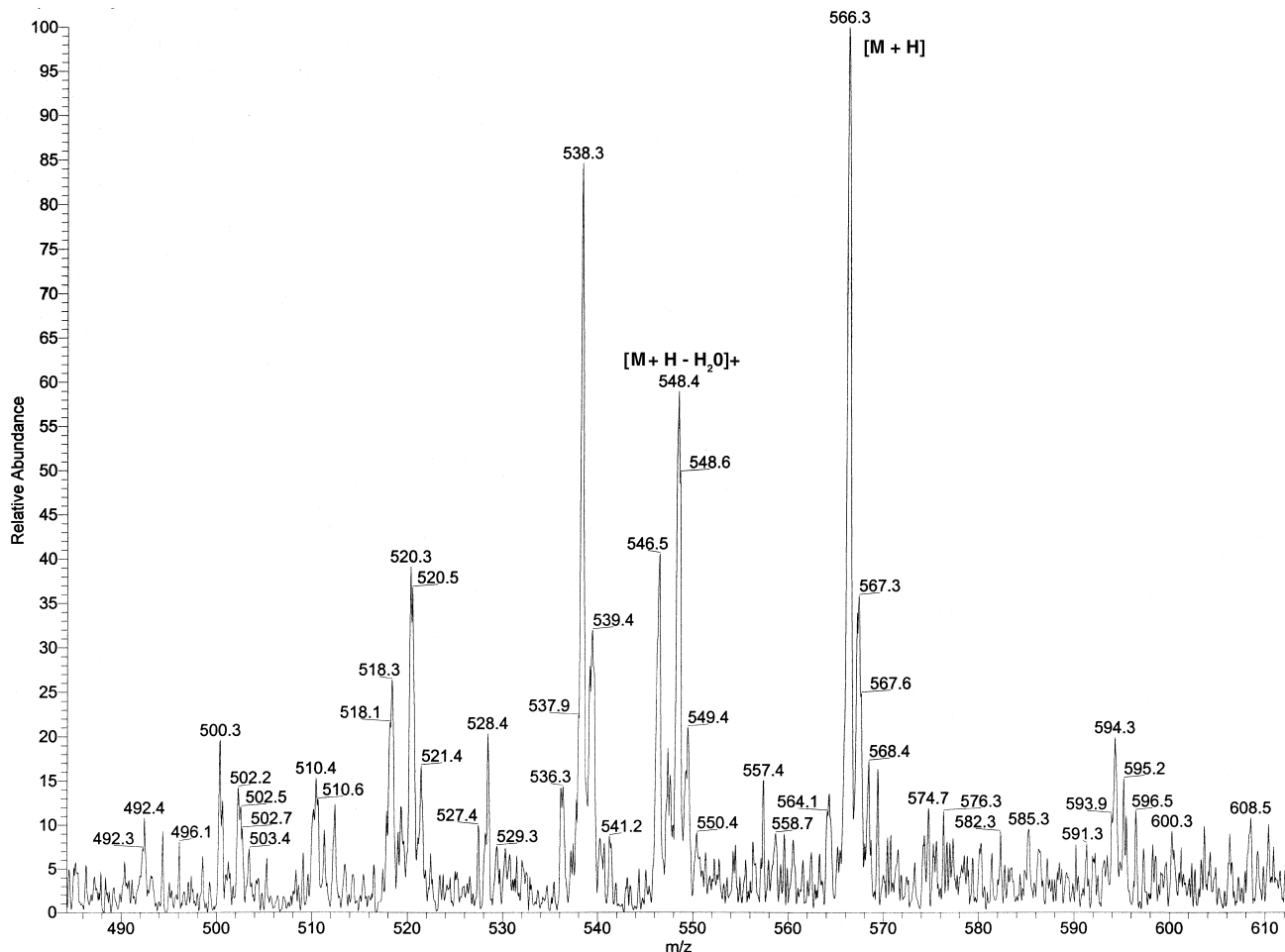


Fig. 1. Electrospray ionization-mass spectrometry of ceramide isolated from *Manduca sexta* larvae. The $[M + H]^+$ peaks of ceramides are at m/z 510, 538, 566, and 594, and their fatty acid chain length varies from C-18, C-20, C-22, and C-24, respectively. The $[M + H - H_2O]^+$ peaks are also observed at m/z 520 and m/z 548 for the more abundant ceramide, with fatty acid chain C-20 and C-22, respectively. Ceramides with extra unsaturation are clearly observed at m/z 518 and m/z 566.

Dephosphorylation of sphingomyelin with sphingomyelinase

Sphingomyelin (10 mg) isolated from *M. sexta* was suspended in 0.1 M phosphate buffer (pH 7.4) and treated with 10 units of sphingomyelinase at 37°C for 18 h. The resultant ceramide was extracted to 2 ml of $CHCl_3$ -MeOH (8:2). The upper layer was discarded, and the lower layer was dried with $MgSO_4$ and filtered through cotton.

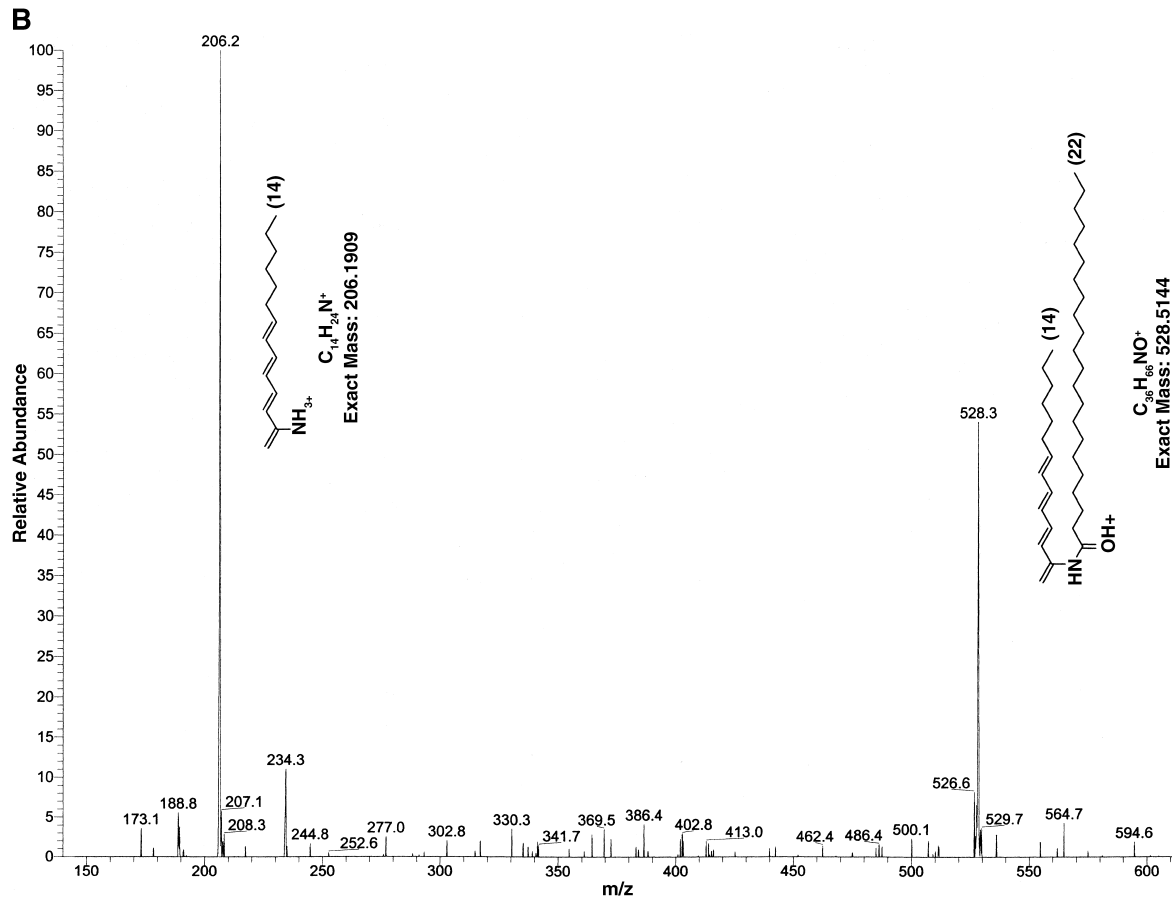
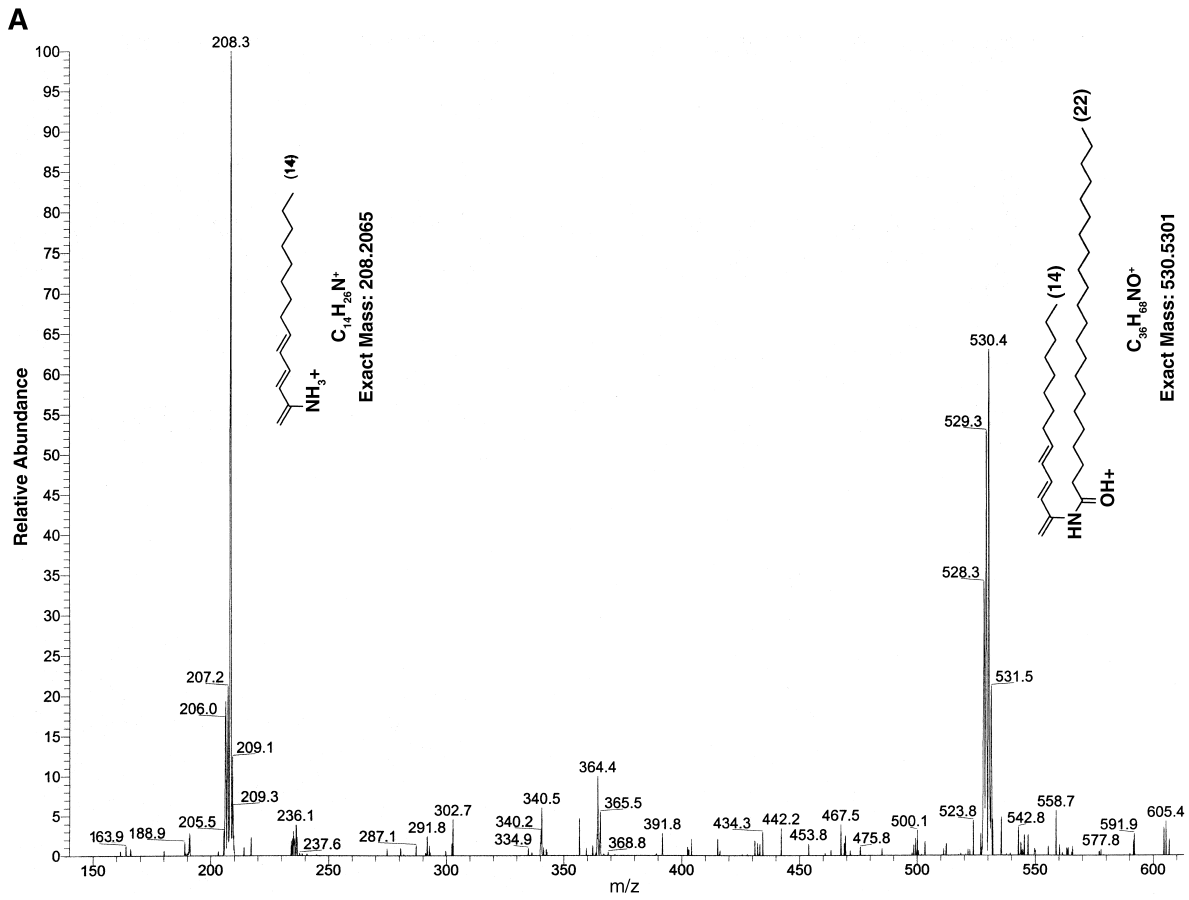
Apoptosis induction using ceramide obtained from *M. sexta*

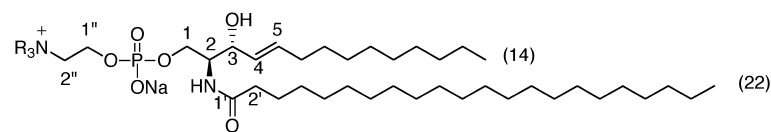
A *Manduca* embryonic cell line (MRRL-CH1) (36) was used to study whether apoptosis can be induced by ceramide obtained from *Manduca*. The embryonic cell line was maintained in 2.5% fetal bovine serum for 2–3 days after seeding the wells of a 12-well plate, then treated with 80 μ M commercial ceramide (Avanti Polar Lipids, Inc., catalog number 860518P) in ethanol, 80 μ M ceramide obtained from sphingomyelin isolated from fifth-instar larvae, and stage 12 metamorphosing adults in ethanol, or ethanol alone as a control for 72 h. Cells were fixed and labeled according to the protocol given by APO-BrdU terminal deoxynucleotidyl transferase-mediated biotin-dUTP nick end labeling (TUNEL) assay kit (Molecular Probes, catalog number

A-23210), except that the centrifugation speed was increased to 735 g, the incubation time for exposure to the DNA-labeling solution was increased to 2 h, and the incubation time for exposure to the anti-BrdU solution was increased to 1 h. Cells from each well were separately mounted on slides and observed under the confocal microscope using appropriate lasers and filters.

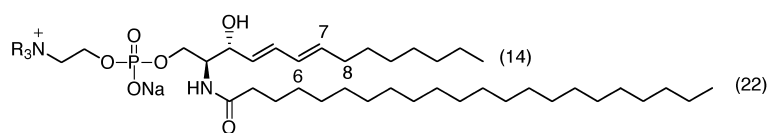
Isolation of lipid rafts

Lipid rafts were isolated using a protocol adapted from several sources (37–39). Twenty-five animals (stage 7, roughly midway through metamorphic adult development) were anaesthetized by cooling on ice. Brains were dissected under insect saline (150 mM NaCl, 4 mM KCl, 6 mM $CaCl_2$, 10 mM HEPES, 5 mM glucose, pH 7.0, adjusted to 360 mOsm with mannitol) (40), frozen in liquid nitrogen, and stored at $-80^\circ C$. The brains were thawed on ice in tris-sodium EDTA (TNE) buffer (25 mM Tris-HCl, 150 mM NaCl, 5 mM EDTA, pH 7.4) containing protease inhibitors (Sigma #P-2714) and homogenized in a Potter-Elvehjem tissue grinder, followed by several passages through a 30 G needle. The homogenate was centrifuged at 4°C in an Eppendorf Model 5415C tabletop centrifuge at 2,000 rpm (~ 325 g) for 10 min. The pellet, which was expected to contain nuclei and other dense material, was stored at $-80^\circ C$. The supernatant was then centrifuged at 11,000 rpm ($\sim 9,880$ g) for 20 min at 4°C in order





R = CH₃: Sphingomyelin 1 Exact mass = 753.5886
 R = H : Ceramide phosphoethanolamine 3 Exact mass = 711.5417



R = CH₃: Sphingomyelin 2 Exact mass = 751.5730
 R = H : Ceramide phosphoethanolamine 4 Exact mass = 709.5260

Fig. 3. Representative structures of sphingomyelin series 1 and 2 and ceramide phosphoethanolamine series 3 and 4. Chain length heterogeneity occurs in both the sphingosine moieties and the fatty acid side chains in all compounds.

to pellet membranes. The resulting supernatant, which was expected to contain soluble proteins, was stored at -80°C . The resulting pellet was resuspended in TNE + protease inhibitors to give 300 μl . To this, 100 μl of TNE containing 2% Triton X-100 was added to give a final Triton concentration of 0.5%. The solution was incubated on ice for 30 min to allow solubilization of nonraft lipid membranes. To this solution, 1.2 ml of 80% sucrose in TNE was added to give a final sucrose concentration of 60%. This was layered into a Beckman Ultraclear 6 ml centrifuge tube and overlaid with 1 ml each of 40, 30, 5, and 0% sucrose in TNE (without Triton). The tube was centrifuged at 2°C for 18 h at 40,500 rpm ($\sim 160,000 g$) in a Beckman LM-8 ultracentrifuge using a SW 50.1 hanging bucket rotor. Nine 600 μl fractions were collected from the top of the tube. To each fraction, 4.4 ml TNE was added to lower the sucrose concentration. The diluted fractions were then spun in the hanging bucket rotor for 30 min at 2°C and 39,000 rpm ($\sim 140,000 g$) to pellet membranes. The pellets were resuspended in 250 μl TNE, transferred to a glass test tube, and extracted into 500 μl of $\text{CHCl}_3\text{-MeOH}$ (2:1). The aqueous and organic phases were processed separately; the white interface was expected to contain amphipathic molecules and was included with the organic phase.

Western blotting of sucrose gradient fractions

Following $\text{CHCl}_3\text{-MeOH}$ extraction, proteins in the aqueous phase were precipitated with cold (-20°C) acetone. Precipitated proteins were solubilized in SDS sample buffer and run out on a 4–12% NuPAGE polyacrylamide gel (Invitrogen), then transferred to polyvinylidene difluoride membrane (0.45 μm , Millipore). The membrane was agitated in Tris-buffered saline (TBST) (100 mM Tris-HCl, 150 mM NaCl, pH 7.5) containing 0.1% Tween 20 (TBST) to block nonspecific protein binding, then incubated overnight at 4°C in guinea pig anti-glycosylphosphatidylinositol (GPI)-Fas (kind gift of Dr. Philip Copenhaver, Oregon Health Sciences University) diluted 2.5:10,000 in TBST (41), washed in TBST, incubated in peroxidase-conjugated donkey anti-guinea pig secondary antibody (2:10,000 in TBST) for 2 h at room temperature, washed in TBST, and visualized with an Opti-4CN substrate kit (Bio-Rad).

Isolation of sphingomyelin from sucrose gradient fractions

The lower (chloroform) layer resulting from the $\text{CHCl}_3\text{-MeOH}$ extraction was evaporated to dryness and treated with 500 μl of 0.1 N NaOH at 45°C for 4 h. After neutralization with 0.1 N HCl, the solutions were desalted on C-18 cartridges (Isolute SPE Part number 221-0100-C) with 5 ml of water. The remaining sucrose was eluted with 5 ml of methanol, and the sphingomyelins were eluted with 5 ml of $\text{CHCl}_3\text{-MeOH}$ (2:1). The structures were confirmed using liquid chromatography-mass spectrometry.

RESULTS

The isolation of sphingosine derivatives from 4-day-old fifth-instar larvae gave the ceramides sphingomyelin and ceramide phosphoethanolamine. The HPLC fraction with a retention time of 5 min contained ceramide, but only enough to study by mass spectrometry. ESI mass spectra of ceramides show the presence of four ceramides, as seen in Fig. 1.

Dehydration of ceramides took place following FAB ionization in the JEOL sector (EB) mass spectrometer, as broad “metastable” peaks were observed at an m/z value of M^* (e.g., 530.6) that is related to the precursor ion mass M_1 (e.g., 566) and fragment ion mass M_2 (e.g., 548) by the relationship $M^* = (M_2)^2/M_1$. Chemical formulae were proven by high-resolution mass spectra obtained using a 4.7T Ionspec FT-ICR spectrometer. FT-ICR gave mainly the $[\text{M} + \text{Na}]^+$ peaks of the precursor ceramides at m/z 532.4714 (calc. 532.4706; $\text{C}_{32}\text{H}_{63}\text{NNaO}_3^+$), 560.5021 (calc. 560.5019; $\text{C}_{34}\text{H}_{67}\text{NNaO}_3^+$), 588.5346 (calc. 588.5332; $\text{C}_{36}\text{H}_{71}\text{NNaO}_3^+$), and 616.5667 (calc. 616.5645; $\text{C}_{38}\text{H}_{75}\text{NNaO}_3^+$). The intensities of the dehydrated ceramides were almost negligible for the above ceramides in the FT-ICR spectra. Collision-induced tandem mass spec-

Fig. 2. Electrospray ionization-mass spectrometry³ fragmentation spectra of $[\text{MH} - \text{H}_2\text{O}]^+$ ions of m/z 530 (A) and m/z 528 (B). In both cases, the $[\text{MH} - \text{H}_2\text{O}]^+$ ions were generated by tandem mass spectrometry from $[\text{M} + \text{H}]^+$. Placement of the H^+ on the fragments is arbitrary. The minor peak at m/z 234 probably represents a small contribution from the C16:0 sphingosine fatty acid coupled with the C20:0 fatty acid.

TABLE 1. Electrospray ionization-mass spectrometry and nth-order tandem mass spectrometry data of ceramide phosphoethanolamine^a

[M + Na] ⁺	[MNa - 43] ⁺	[MNa - 43 - 98] ⁺	[MNa - 43 - 98 - 22 - 18] ⁺	[Sphingosine Fragment] ⁺	[Fatty Acid Fragment] ⁺
681	638	540	500	206	336
683	640	542	502	208	336
709	666	568	528	206	364
711	668	570	530	208	364

^aPeak positions are in daltons.

tra MSⁿ (n = 2–4) were obtained for each of the ceramides to identify the chain length of the sphingosine and the fatty acid in the ceramides, as shown in **Fig. 2**.

HPLC fractions with a retention time of 19 min were evaporated to dryness with a rotary evaporator, and the ¹H NMR spectroscopic data were recorded in CDCl₃-CD₃OD-D₂O (1:1:0.1) at 298°C. ¹H NMR: 5.73 (dd, 1H, J = 15.0, 7.0, H-5), 5.44 (dd, 1H, J = 8.0, 15.0, H-4), 4.03 (m, H-1"), 4.16 (m, H-1), 4.08 (t, 1H, J = 8, H-3), 3.90 (m, H-1), 3.91 (m, H-2), 3.11 (t, 2H, J = 5.0, H-2"), 2.18 (t, 2H, J = 7.5, H-2'), 2.02 (t, 2H, J = 7.3, H-6), 1.35–1.25 (m), 0.90 (t). ¹³C NMR from HSQC experiment: 134.8 (C-5), 129.6 (C-4), 71.6 (C-3), 65.0 (C-1), 62.7 (C-1"), 54.3 (C-2), 41.0 (C-2"), 37.0 (C-2'), 33.0 (C-6), 26.6 (C-3'), 23.1 (C-7), 30.0 (CH₂), 14.2 (CH₃).

This fraction contained ceramide phosphoethanolamine, and according to ¹H NMR, it contained two types of phosphoethanolamines (**Fig. 3**). The normal set of ceramide phosphoethanolamine (compound **3**) also varied at the fatty acid attached to the ceramide. The [M + Na]⁺ peaks of the different ceramide phosphoethanolamines were observed at *m/z* 655, 683, 711, and 739. FT-ICR was used to obtain the high-resolution mass spectra, and the results are 655.4773 (calc. 655.4791; C₃₄H₆₉N₂NaO₆P⁺), 683.5097 (calc. 683.5104; C₃₆H₇₃N₂NaO₆P⁺), 711.5406 (calc. 711.5417; C₃₈H₇₇N₂NaO₆P⁺), and 739.5717 (calc. 739.5730; C₄₀H₈₁N₂NaO₆P⁺).

The chain length of ceramide phosphoethanolamine was obtained using ESI-MSⁿ data. In the case of sodiated ceramide phosphoethanolamine, ESI-MS/MS data result in loss of 43 (terminal ethylene amine) followed by the rest of the phosphate group as a fragment of 98. For example, ceramide phosphoethanolamine at *m/z* 683 [M + Na]⁺ initially gave a fragment at *m/z* 640. Further fragmentation of *m/z* 640 resulted *m/z* 542. In the same spectrum, a peak at *m/z* 520 is observed, which is the protonated peak of *m/z* 542. The [MH - H₂O]⁺ peak of *m/z* 520 was observed at *m/z* 502. Upon mass selection of *m/z* 502, the C-14 sphingosine chain gave a peak at *m/z* 208, and the fatty acid gave a fragment at *m/z* 336, corresponding to a fatty acid chain length of 20 carbons. All results are tabulated in **Table 1**.

It is interesting to note that the presence of doubly unsaturated ceramide is also seen in the ceramide phosphoethanolamine, and that the C14/20 and C14/22 ceramides were the most abundant species present. The high-resolution mass spectra data for [M + Na]⁺ are 681.4938 (calc. 681.4947; C₃₆H₇₁N₂NaO₆P⁺) and 709.5250 (calc. 709.5260; C₃₈H₇₅N₂NaO₆P⁺). As will be discussed later in more de-

tail, the proton NMR spectra clearly showed the presence of the doubly unsaturated partner, and correlation spectroscopy (COSY) helped identify the connectivity.

Fractions with retention times of 32 and 33 min were evaporated to dryness, and spectroscopic data were recorded in CDCl₃-CD₃OD-D₂O (1:1:0.1) at 305°C. ¹H NMR: 5.71 (dd, 1H, J = 15.5, 7.0, H-5), 5.45 (dd, 1H, J = 8.0, 15.5, H-4), 4.28 (m, H-1"), 4.15 (m, H-1), 4.07 (t, 1H, J = 8, H-3), 3.93 (m, H-1), 3.91 (m, H-2), 3.61 (t, 2H, J = 4.5, H-2"), 3.25 [9H, s, N⁺(CH₃)₃], 2.18 (t, 2H, J = 7.3, H-2'), 2.02 (t, 2H, J = 7.3, H-6), 1.35–1.25 (m), 0.90 (t). ¹³C NMR from HSQC experiment: 134.8 (C-5), 129.7 (C-4), 71.5 (C-3), 66.8 (C-2"), 65.0 (C-1), 59.6 (C-1"), 54.2 (C-2), 54.4 [N⁺(CH₃)₃], 37.0 (C-2'), 33.0 (C-6), 26.7 (C-3'), 23.1 (C-7), 30.0 (CH₂), 14.2.

Two types of sphingomyelins were isolated from the lipid extract of *M. sexta*. The normal set of sphingomyelin (compound **1**) varies from the fatty acid attached to the ceramide. ESI-mass spectrometry data gave the [M + Na]⁺ peaks at *m/z* 697, 725, 753, and 781. The chemical formulae for [M + H]⁺ of the different sphingomyelins were confirmed using FT-ICR as 675.5487 (calc. 675.5441; C₃₇H₇₆N₂O₆P⁺), 703.5770 (calc. 703.5754; C₃₉H₈₀N₂O₆P⁺), 731.6088 (calc. 731.6067; C₄₁H₈₄N₂O₆P⁺), and 759.6442 (calc. 759.6380; C₄₃H₈₈N₂O₆P⁺).

Attempts were made to obtain the chain lengths of sphingomyelin using ESI-MSⁿ in the same way as was done for ceramides. As the isolated sphingomyelin exists mainly in the sodiated form, it loses 59 mass units (trimethyl amine) and 124 (rest of the phosphocholine group). In FAB, the whole phosphocholine group loses as a fragment with mass of daltons 184. However, the corresponding protonated ceramide fragment of [MH - 59 - 124 - 18]⁺ can be used to obtain chain length information as in the case of ceramide phosphoethanolamine.

In addition to ESI-MSⁿ measurement in the IT instrument, ESI-CID on a triple quadrupole instrument was also

TABLE 2. CID fragments in daltons of sphingomyelins **1** in the triple quadrupole instrument

Molecular Mass	[M + Li] ⁺	Sphingosine Fragment		Fatty Acid Fragment
		C-14	C-16	
674	681	208	236	308, 280
702	709	208	—	336
730	737	208	—	364
758	765	208	236	392, 364

CID, collision-induced dissociation.

TABLE 3. CID fragments of sphingomyelins **2** in the triple quadrupole instrument

Molecular Ion	(M + Li) ⁺	Sphingosine Fragment		Fatty Acid Fragment
		C-14	C-16	
700	707	206	—	336
728	735	206	234	364, 336

used to obtain chain length information. In these experiments, LiOAc was added to the medium because the lithiated sphingomyelins fragmented more efficiently on the triple quadrupole instrument. Mass selecting m/z 737.5 [(compound **1**) + Li⁺] and fragmentation with a collision energy of 50 eV gave two major fragments (42) at m/z 208 and m/z 364, which provides information on the sphingosine chain length and the fatty acid chain length, respectively. The sphingosine and the fatty acid in the ceramide were identified as tetradecasphing-4-ene and behenic acid, respectively. The identity of all sphingomyelins was obtained from the tandem mass experiments by mass selection of the desired lithiated precursor ion. The results are tabulated in **Table 2**.

It was concluded that the sphingosine in all compounds was tetradecasphing-4-ene, and the acids are stearic, arachidic, behenic and lignoceric. Yet, two sphingomyelins with molecular mass of 674 daltons and 758 daltons showed heterogeneity in the ceramide backbone, shown as italicized numbers in Table 2. The sphingosine fragment at m/z 236 corresponds to the hexadecasphing-4-ene. The corresponding fatty acid fragment without two methylenes was also observed, confirming the above conclusion.

The second set of sphingomyelins (compound **2**) is novel, in that it contains an additional double bond at C-6 of the sphingosine. The chemical formulae for [M + H]⁺ of this set of sphingomyelins were confirmed using high-resolution FAB mass spectrometry as 673.5253, 701.5581, 729.5905, and 757.6566 daltons. ESI-CID-MS/MS of the lithiated molecular ion at m/z 735.5 gave fragments at m/z 206 and m/z 364 (**Table 3**). Hence, it was determined that the unusual double bond is located on the sphingoid base, and that the fatty acid is saturated. The relative

abundance of the sphingomyelins is shown in brackets 672 (3.1), 674 (24.1), 700 (32.3), 702 (100.0), 728 (23.4), 730 (67.8), 756 (5.6), and 758 (15.1). Tandem mass experiments were not possible on the molecular ions at [672 + Li]⁺ and [756 + Li]⁺ due to their low intensities.

The position of the unusual unsaturation in sphingomyelin **2** and ceramide phosphoethanolamine **4** was confirmed by COSY. Correlation of the protons 3, 4, 5, 6, 7, and 8 (labeled in Fig. 3) was clearly identifiable in the cross peaks. The sphingosine was identified as tetradecasphing-4,6-dienine. It is noteworthy that each “normal” sphingomyelin is accompanied by its doubly unsaturated counterpart. The ¹H NMR chemical shifts of the two types of sphingomyelins and the two types of ceramides ethanolamine are tabulated in **Table 4**.

The ¹H NMR chemical shift of the methine proton at H-3 depends on the C-3 configuration of the sphingosine backbone, with H-3 shifted downfield by 0.28 δ (4.44 δ *threo* vs. 4.05 δ *erythro*) for the *threo* compound (43). The ¹H NMR spectrum of sphingomyelin **1** was obtained in CD₃OD, and H-3 was located at 4.04 δ. Based on these results, the *erythro* configuration was assigned to **1**. In the ¹³C spectra, a chemical shift difference (Δδ) of 5.0 ppm for the carbons C-4 and C-5 is regarded as an indication of the *erythro* configuration of the sphingolipid, while Δδ = 4.0 ppm indicates the *threo* configuration (44). Sphingosine **1** has Δδ = 5.1 ppm for C-4 and C-5, consistent with the *erythro* configuration.

Ceramide ethanolamine and sphingomyelin were also isolated from stage 12 metamorphosing adult. The ratio between sphingomyelin **1:2** is different in stage 12 metamorphosing adult and fifth-instar larvae according to ¹H NMR (**Fig. 4**) as well as high-resolution mass spectral data.

Ceramide obtained from the hydrolysis of sphingomyelin contained the expected C-14/18, C-14/20, C-14/22, and C-14/24 chain lengths in the sphingosine and the fatty acid chain. The doubly unsaturated ceramide was also observed and the position of the double bond was proven by mass spectra and NMR as explained before. Preliminary results using a TUNEL assay showed apoptotic cells (**Fig. 5**) in wells treated with ceramides obtained from fifth-instar larvae and stage 12 metamorphosing adult at a concentration of 80 μM. Commercial ceramide did not induce apoptosis at this concentration.

TABLE 4. ¹H NMR data of sphingomyelins **1** and **2** and ceramide phosphoethanolamines **3** and **4** in CDCl₃-CD₃OD-D₂O (1:1:0.1) at 305°C

Position	Sphingomyelin 1		Ceramide Phosphoethanolamine 3		Sphingomyelin 2		Ceramide Phosphoethanolamine 4	
	¹ H (δ)	J (Hz)	¹ H (δ)	J (Hz)	¹ H (δ)	J (Hz)	¹ H (δ)	J (Hz)
1	4.15, 3.93 m		4.16, 3.90 m		4.15, 3.93 m		4.16, 3.90 m	
2	3.91 m		3.91 m		3.91 m		3.91	
3	4.07 t	8.0	4.08 t	8.0	4.12 m		4.15 m	
4	5.45 dd	8.0, 15.5	5.44 dd	8.0, 15.0	5.53 dd	7.5, 15.5	5.53 dd	7.5, 15.0
5	5.71 dd	7.0, 15.5	5.73 dd	7.0, 15.0	6.21 dd	10.5, 15.5	6.21 dd	10.5, 15.5
6	2.02 t	7.3	2.02 t	7.3	6.01 dd	10.5, 15.5	6.01 dd	10.5, 15.0
7	1.36 m		1.36 m		5.72 dd	6.5, 15.5	5.69 dd	7.5, 15.0
8					2.06 t	6.5	2.06 t	7.5

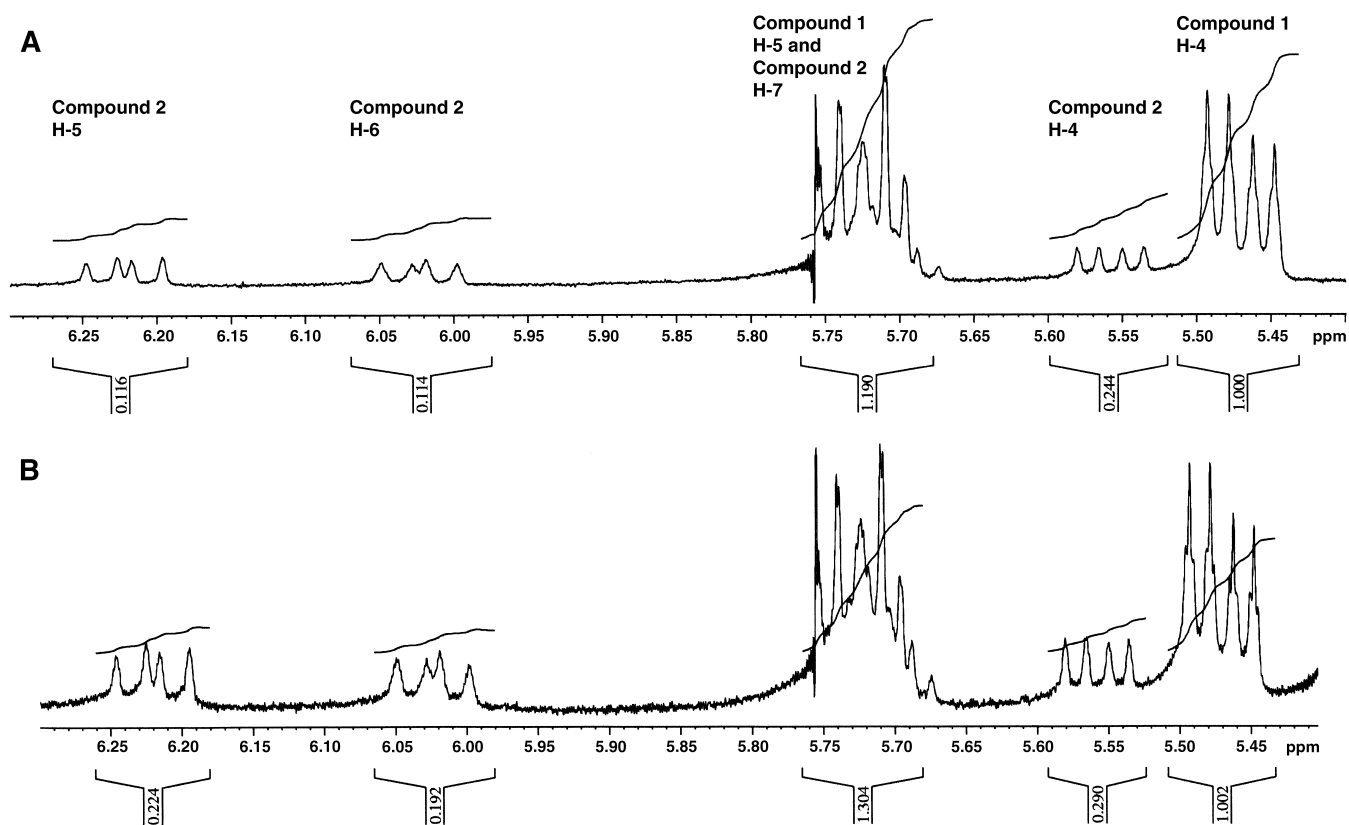


Fig. 4. ^1H NMR spectra (olefinic region) of sphingomyelins **1** and **2** shown in Fig 3. A: Sphingomyelin isolated from stage 12 metamorphosing adult. B: Sphingomyelin isolated from fifth-instar larvae.

A Western blot of sucrose gradient fractions (nine 600 μl fractions) was done to test for the presence of GPI-linked *Manduca* fasciclin II (GPI-MfasII) in the fractions. GPI-linked proteins are known to be concentrated in lipid

rafts in both vertebrates and invertebrates (31, 32), so the presence of GPI-MfasII can serve as a marker for lipid rafts in isolated fractions. The blot (**Fig. 6**) indicates that lipid rafts would likely be found in fractions 3 and 4,

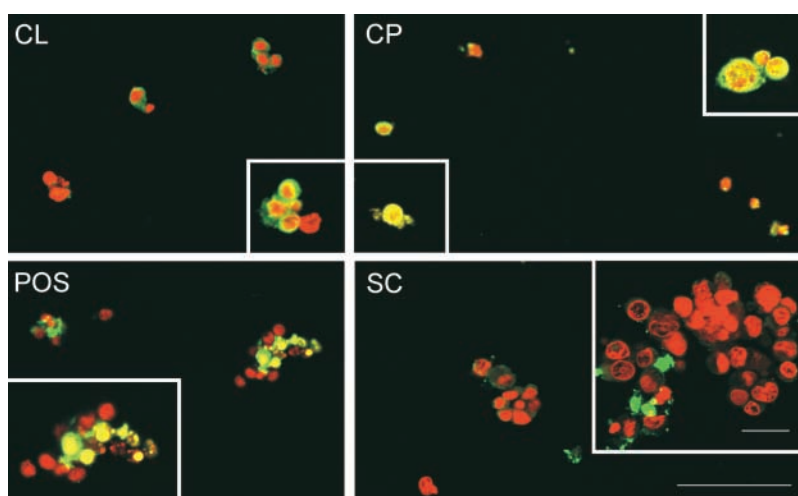


Fig. 5. Terminal deoxynucleotidyl transferase-mediated biotin-dUTP nick end labeling (TUNEL) assay on embryonic *Manduca* cells (MRRL-CHI) treated with ceramide obtained from fifth-instar larvae (CL), from stage 12 metamorphosing adults (CP), or with commercially available ceramide (SC). POS, cells in positive control population supplied in the TUNEL kit; red, cell nuclei, labeled with the nucleic acid stain propidium iodide; green, cells labeled with BrdUTP and terminal deoxynucleotidyl transferase and visualized with anti-BrdU-Alexa-488 to indicate the presence of the DNA strand breaks characteristic of apoptosis. Apoptotic cells have yellow nuclei. Some of the cells in the CL and CP conditions were undergoing apoptosis; none were found after treatment with standard ceramide at a concentration of 80 μM . Scale bar for low-power views = 100 μm ; for insets = 25 μm .

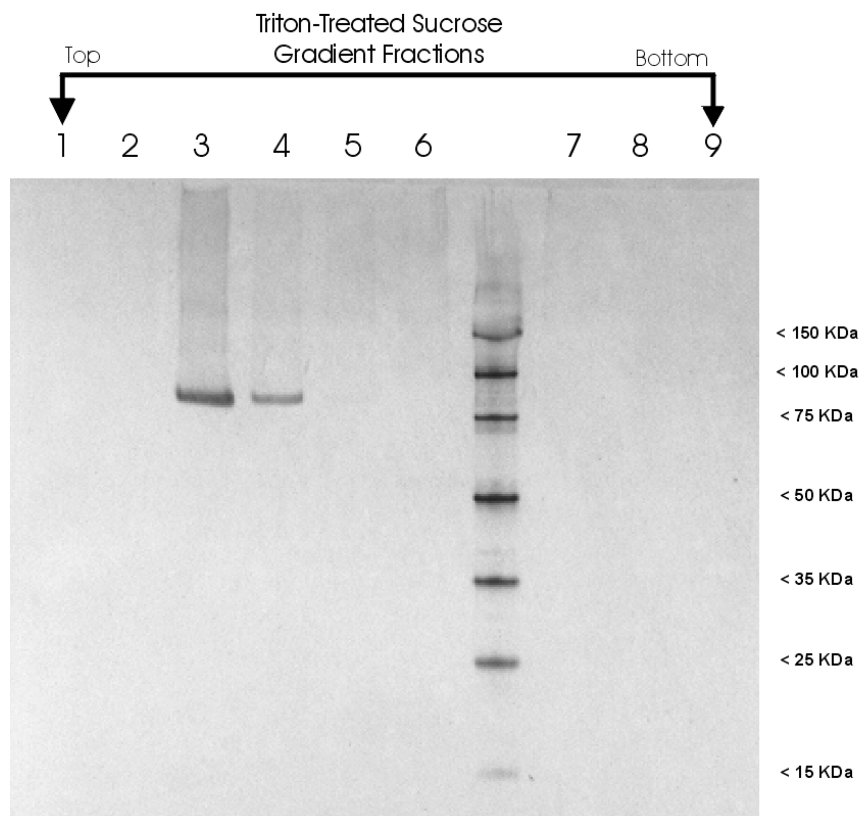


Fig. 6. Western blot using an antibody to glycosylphosphatidylinositol-Fas (GPI-Fas), an *M. sexta* protein expected to be localized to lipid rafts (by virtue of its GPI anchor), detects the protein associated with fractions 3 and 4. These fractions were also the ones found to contain sphingomyelin, suggesting that the sphingomyelin was indeed a component of lipid rafts.

which were removed from the gradient from the region originally corresponding to 30% sucrose.

The CHCl_3 -MeOH extract of lanes 3–4 contains two major peaks at m/z 725 and m/z 753 mass units in the ESI-MS corresponding to sodiated sphingomyelins. Secondary ion mass spectra give peaks at 208 for both sphingomyelins. It is also interesting to note the presence of m/z 723 and m/z 751 corresponding to the doubly unsaturated sphingomyelin. The amount of this diene is only 4% of the natural sphingomyelin, however.

DISCUSSION

Ceramides isolated from *M. sexta* larvae had molecular mass of 509, 537, 565, and 593 daltons with 16:85:100:21 relative abundance, respectively. The same mass spectrum shows the presence of the dehydrated form of ceramide for the two most abundant ceramides, and their $[\text{M} + \text{H}]^+$ peaks were observed at m/z 520 and m/z 538. The molecular weights of the ceramides in the larvae vary as the fatty acid attached to the ceramide changes. The chain lengths of the ceramides were obtained using MS/MS/MS data (Fig. 2A). Sphingosine chain length can easily be obtained using the Finnigan LCQ by selecting the $[\text{MH} - \text{H}_2\text{O}]^+$ peak of the original ceramide. The peak at m/z 208

corresponds to the sphingosine chain length with 14 carbons; hence the ceramide in *M. sexta* varies in fatty acid chain length from C-18 to C-24.

Interestingly, these ceramides are accompanied by another ceramide homolog with an unusual diene moiety in the sphingosine chain. It is clearly seen at m/z 546 and m/z 548 in the mass spectrum (Fig. 1); hence, $[\text{MH} - \text{H}_2\text{O}]^+$ peaks were used in the MS/MS/MS experiments to prove the sphingosine chain length. To illustrate this further, the ceramide with the additional unsaturation (m/z 564, Fig. 1) produces a $[\text{MH} - \text{H}_2\text{O}]^+$ peak at m/z 546. MS/MS of m/z 546 provided a peak at m/z 528 owing to the loss of a second water molecule. MS/MS/MS of m/z 528 gave a peak at m/z 206 (Fig. 2B), not at m/z 208, indicating that the additional unsaturation is on the sphingosine chain.


M. sexta contains two types of ceramide phosphoethanolamines. The most abundant ceramide phosphoethanolamine possesses a C-14 sphingosine chain, and the fatty acid chain length varies from C-18 to C-24. The novel ceramide phosphoethanolamine has additional unsaturation in the sphingosine chain as seen by CID data (Table 1). The ratio of the two compounds 3:4 is about 20% by NMR and is the same in the larvae and metamorphosing adults.

Four-day-old, fifth-instar larvae of *M. sexta* contain at least two types of sphingomyelins that have not been previously identified in this insect. This information is interesting

from a taxonomical viewpoint, inasmuch as sphingomyelin has not been previously identified in any *Lepidopteran* species. Sphingomyelin has been previously isolated from *Coleoptera* (4), but not from *Diptera*. The sphingomyelins in *Coleoptera* were not reported to contain the novel unsaturated sphingoid base reported here.

The extracts of the stage 12 metamorphosing adult did not contain ceramides but did contain sphingomyelin series 1 and 2. However, the ratio of compounds 1:2 was clearly changed according to the NMR. Five-day-old fifth-instar larvae contain 20% of compound 2 as opposed to compound 1, whereas the stage 12 metamorphosing adult contains only 10% of compound 2. Similar experiments show that the stage 17–18 metamorphosing adult contains 20% of compound 2. To further confirm the identity of compound 2 and to study the ceramide-induced apoptosis, the sphingomyelin mixture was subjected to enzymatic digestion with sphingomyelinase, which cleaves the phosphocholine head group of sphingomyelin. NMR data and mass spectra confirm the presence of the ceramide with extra unsaturation.

The TUNEL assay was used as one measure of whether ceramide might induce apoptosis in cells from an embryonic *Manduca* cell line. The results provided initial evidence suggesting that the ceramide mixture obtained from stage 12 *M. sexta* is more effective in inducing apoptosis than the commercial ceramide lacking extra unsaturation, supporting the hypothesis that the extra unsaturation at C-6 of the sphingosine enhances apoptosis. Further work will be required to confirm this hypothesis.

In addition to investigating the possible role of sphingomyelin in apoptosis, we also investigated its possible role in forming lipid rafts, specialized membrane domains rich in sterols, sphingomyelin, and GSLs. Lipid rafts are known to function as platforms that concentrate GPI-linked proteins, receptor tyrosine kinases, GTPases, and SNARE and SNAP proteins (elements essential to synaptic function) (29–31). GPI-MfasII was found in sucrose gradient fractions 3 and 4 obtained from stage 7 brains following Triton solubilization. These were the same fractions from which sphingomyelins were isolated. This association strongly suggests that the sphingomyelins are indeed components of lipid rafts. Sphingomyelins were found in fractions 3 and 4, and the structures were confirmed using mass spectra. The most abundant ceramides in those sphingomyelins had a C-14 sphingosine chain and C-20 and C-22 fatty acyl chains. The doubly unsaturated compound was also observed in the sphingomyelins extracted from fractions 3 and 4. 

The authors thank the U.S. Army (DAMD 17-99-1-9539) for financial support and the National Science Foundation (CHE-9601809, CHE-9729350) for purchase of the Sector mass spectrometry instrument and the 500 MHz Bruker NMR. N.J.G. and L.A.O. were supported by National Institutes of Health Grant P01-NS-28495. Special thanks go to Dr. George Tsprallis of the Mass Spectrometry Facility of the Pharmacy Department, University of Arizona, for the use of the TSQ 7000 instrument and to Dr. Roy H. Hammerstedt of Matreya, Inc.

REFERENCES

1. Reinisova, J., and C. Michalec. 1966. Biochemistry of sphingolipids-X. Comparative study of sulfatides and cerebrosides in brain tissues of various animals. *Comp. Biochem. Physiol.* **19**: 581–588.
2. Bieber, L. L., J. D. O'Connor, and C. C. Sweeley. 1969. The occurrence of tetradecasphing-4-enine and hexadecasphing-4-enine as the principal sphingosines of *Musca domestica* larvae and adults. *Biochim. Biophys. Acta.* **187**: 157–159.
3. Dawson, R. M. C., and P. Kemp. 1968. Isolation of ceramide phosphorylethanolamine from the blowfly *Calliphora erythrocephala*. *Biochem. J.* **106**: 319–320.
4. Rao, K. D. P., and H. C. Agarwal. 1969. Lipids of the larvae and adult of *Trogoderma granarium* (Coleoptera). *Comp. Biochem. Physiol.* **30**: 161–167.
5. Karlander, S. G., K. A. Karlsson, H. Leffler, A. Lilja, B. E. Samuelson, and G. O. Steen. 1972. The structure of sphingomyelin of the Honey bee (*Apis mellifera*). *Biochim. Biophys. Acta.* **270**: 117–131.
6. Luukkonen, A., M. Brummer-Korvenkontio, and O. Renkonen. 1973. Lipids of cultured mosquito cells (*Aedes albopictus*). Comparison with cultured mammalian fibroblasts (BHK 21 cells). *Biochim. Biophys. Acta.* **326**: 256–261.
7. Butters, T. D., and R. C. Hughes. 1981. Phospholipids and glycolipids in subcellular fractions of mosquito *Aedes aegypti* cells. *Natl. Inst. Med. Res. London. Engl.* **17**: 831–838.
8. Sugita, M., M. Nishida, and T. Hori. 1982. Studies on glycosphingolipids of larvae of the green-bottle fly, *Lucilia caesar*. I. Isolation and characterization of glycosphingolipids having novel sugar sequences. *J. Biochem. (Tokyo).* **92**: 327–334.
9. Dennis, R. D., R. Geyer, H. Egge, H. Menges, S. Stirn, and H. Wiegand. 1985. Glycosphingolipids in insects. Chemical structures of ceramide monosaccharide, disaccharide, and trisaccharide from pupae of *Calliphora vicina* (Insecta: Diptera). *Eur. J. Biochem.* **146**: 51–58.
10. Seppo, A., M. Moreland, H. Schweingruber, and M. Tiemeyer. 2000. Zwitterionic and acidic glycosphingolipids of the *Drosophila melanogaster* embryo. *Eur. J. Biochem.* **267**: 3549–3558.
11. Chatterjee, S. 1998. Sphingolipids in atherosclerosis and vascular biology. *Arterioscler. Thromb. Vasc. Biol.* **18**: 1523–1533.
12. Hobson, J. P., H. M. Rosenfeldt, L. S. Barak, A. Olivera, S. Poulton, M. G. Caron, S. Milstien, and S. Spiegel. 2001. Role of the sphingosine-1-phosphate receptor EDG-1 in PDGF-induced cell motility. *Science.* **291**: 1800–1803.
13. Wiegand, H. 1992. Insect glycolipids. *Biochim. Biophys. Acta.* **1123**: 117–126.
14. Kinsella, J. E. 1969. The lipids of *Lepisma saccharina* L. *Lipids.* **4**: 299–300.
15. Ogg, C. L., and D. Stanley-Samuelson. 1992. Phospholipid and triacylglycerol fatty acid compositions of the major life stages and selected tissues of the tobacco hornworm *Manduca sexta*. *Comp. Biochem. Physiol. B: Comp. Biochem.* **101B**: 345–51.
16. Hsu, F-F., and J. Turk. 2000. Structural determination of sphingomyelin by tandem mass spectrometry with electrospray ionization. *J. Am. Soc. Mass Spectrom.* **11**: 437–449.
17. Pettus, B. J., C. E. Chalfant, and Y. A. Hannun. 2002. Ceramide in apoptosis: an overview and current perspectives. *Biochim. Biophys. Acta.* **1585**: 114–125.
18. Ji, L., G. Zhang, S. Uematsu, Y. Akahori, and Y. Hirabayashi. 1995. Induction of apoptotic DNA fragmentation and cell death by natural ceramide. *FEBS Lett.* **358**: 211–214.
19. Hartfield, P. J., G. C. Mayne, and A. W. Murray. 1997. Ceramide induces apoptosis in PC12 cells. *FEBS Lett.* **401**: 148–152.
20. Ping, S. E., and G. L. Barrett. 1998. Ceramide can induce cell death in sensory neurons, whereas ceramide analogues and sphingosine promote survival. *J. Neurosci. Res.* **54**: 206–213.
21. Radin, N. S. 2001. Apoptotic death by ceramide: will the real killer please stand up? *Med. Hypotheses.* **57**: 96–100.
22. Corda, S., C. Laplace, E. Vicaut, and J. Duranteau. 2001. Rapid reactive oxygen species production by mitochondria in endothelial cells exposed to tumor necrosis factor- α is mediated by ceramide. *Am. J. Respir. Cell Mol. Biol.* **24**: 762–768.
23. Sullards, M. C., D. V. Lynch, A. H. Merrill, and J. Adams. 2000. Structure determination of soybean and wheat glucosylceramides by tandem mass spectrometry. *J. Mass Spectrom.* **35**: 347–353.
24. Noda, N., R. Tanaka, K. Miyahara, and T. Kawasaki. 1993. Isolation and characterization of a novel type of glycosphingolipid from *Neanthes diversicolor*. *Biochim. Biophys. Acta.* **1169**: 30–38.

25. Nagle, D. G., W. C. McClathey, and W. H. Gerwick. 1992. New glycosphingolipids from the marine sponge *Halichondria panicea*. *J. Nat. Prod.* **55**: 1013–1017.
26. Kwon, H. C., K. C. Lee, O. R. Cho, I. Y. Jung, S. Y. Cho, S. Y. Kim, and K. R. Lee. 2003. Sphingolipids from *Bombycis Corpus 101A* and their neurotrophic effects. *J. Nat. Prod.* **66**: 466–469.
27. Chun, J., G. Li, H. Byun, and R. Bittman. 2002. Synthesis of new trans double-bond sphingolipid analogues: $\Delta^{4,6}$ and Δ^6 ceramides. *J. Org. Chem.* **67**: 2600–2605.
28. He, L., H. Byun, J. Smit, J. Wilschut, and R. Bittman. 1999. Enantioselective synthesis of a novel trans double bond ceramide analogue via catalytic asymmetric dihydroxylation of an enyne. The role of the trans double bond of ceramide in the fusion of Semliki forest virus with target membranes. *J. Am. Chem. Soc.* **121**: 3897–3903.
29. Lee, A. 2001. Membrane structure. *Curr. Biol.* **11**: R811–R814.
30. Simons, K., and E. Ikonen. 1997. Functional rafts in cell membranes. *Nature.* **387**: 569–572.
31. Brown, D. A., and E. London. 1998. Functions of lipid rafts in biological membranes. *Annu. Rev. Cell Dev. Biol.* **14**: 111–136.
32. Hooper, N. M. 1999. Detergent-insoluble glycosphingolipid/cholesterol-rich membrane domains, lipid rafts and caveolae. *Mol. Membr. Biol.* **16**: 145–156.
33. Tsui-Pierchala, B. A., M. Encinas, J. Milbrandt, and E. M. Johnson, Jr. 2002. Lipid rafts in neuronal signaling and function. *Trends Neurosci.* **25**: 412–417.
34. Liour, S. S., and R. K. Yu. 2002. Differential effects of three inhibitors of glycosphingolipid biosynthesis on neuronal differentiation of embryonal carcinoma stem cells. *Neurochem. Res.* **27**: 1507–1512.
35. Sanes, J. R., and J. G. Hildebrand. 1976. Origin and morphogenesis of sensory neurons in an insect antenna. *Dev. Bio.* **51**: 300–319.
36. Eide P. E., J. M. Caldwell, and E. P. Marks. 1975. Establishment of two cell lines from embryonic tissue of the tobacco hornworm, *Manduca sexta* (L.). *In Vitro.* **11**: 395–399.
37. Rietveld, A., S. Neutz, K. Simons, and S. Eaton. 1999. Association of sterol- and glycosylphosphatidylinositol-linked proteins with *Drosophila* raft lipid microdomains. *J. Biol. Chem.* **274**: 12049–12054.
38. Zhuang, M., D. I. Oltean, I. Gomez, A. K. Pullikuth, M. Soberon, A. Bravo, and S. S. Gill. 2002. *Heliothis virescens* and *Manduca sexta* lipid rafts are involved in CryIA toxin binding to the midgut epithelium and subsequent pore formation. *J. Biol. Chem.* **277**: 13863–13872.
39. Hering, H., C. C. Lin, and M. Sheng. 2003. Lipid rafts in the maintenance of synapses, dendritic spines, and surface AMPA receptor stability. *J. Neurosci.* **23**: 3262–3271.
40. Hayashi, J. H., and J. G. Hildebrand. 1990. Insect olfactory neurons in vitro: morphological and physiological characterization of cells from the developing antennal lobes of *Manduca sexta*. *J. Neurosci.* **10**: 848–859.
41. Higgins, M. R., N. J. Gibson, P. A. Eckholdt, A. Nighorn, P. F. Copenhaver, J. Nardi, and L. P. Tolbert. 2002. Different isoforms of fasciclin II are expressed by a subset of developing olfactory receptor neurons and by olfactory-nerve glial cells during formation of glomeruli in the moth *Manduca sexta*. *Dev. Biol.* **244**: 134–154.
42. Karlsson, A. A., P. Michelsen, and G. Odham. 1998. Molecular species of sphingomyelin: determination by high-performance liquid chromatography/mass spectrometry with electrospray and high-performance liquid chromatography/tandem mass spectrometry with atmospheric pressure chemical ionization. *J. Mass Spectrom.* **33**: 1192–1198.
43. Bruzik, K. S. 1988. Conformation of the polar headgroup of sphingomyelin and its analogues. *Biochim. Biophys. Acta.* **939**: 315–326.
44. Bruzik, K. S. 1988. Synthesis and spectral properties of chemically and stereochemically homogeneous sphingomyelin and its analogues. *J. Chem. Soc. Perkins Transactions I.* 423–431.